

# Tensile Yield Behavior of PP/SEBS Blends

A. K. GUPTA and S. N. PURWAR, *Centre for Materials Science and Technology, Indian Institute of Technology, New Delhi-110 016, India*

## Synopsis

Tensile yield behavior of the blends of polypropylene (PP) and styrene-ethylene butylene-styrene block copolymer (SEBS) is studied in blend composition range 0–25 wt % SEBS. Three sets of samples, (i) solution-blended compression-molded (SBCM), (ii) melt-blended compression-molded (MBCM), and (iii) melt-blended injection-molded (MBIM), were studied to investigate the relative merits of solution blending and melt blending and the effect of subsequent mixing during injection moulding. Systematic changes with varying blend composition were found in stress-strain behavior in the yield region, viz., in yield stress, yield strain, width of yield peak, and work of yield. Growth of shear bands before necking also showed some systematic variation with blend composition. Shapes and sizes of dispersed-phase (SEBS) domains at various blend compositions were studied by scanning electron microscopy. Analysis of yield stress data on the basis of the various expressions of first power and two-thirds power laws of blend composition dependence and the porosity model (i.e., the exponential law) led to consistent results from all expressions about the variation of stress concentration effect in these sample sets; the stress concentration effect increased in the following order: MBIM < SBCM < MBCM. Furthermore, in addition to revealing relative suitability of the various expressions to the present system, this analysis also showed a transition around the blend composition 5 wt % SEBS from a continuous to a discontinuous structure. Solution blending produces lower degree of discontinuity in the structure of this two-phase blend than the melt blending, and this discontinuity in melt blended samples is reduced on subsequent mixing during injection-molding process.

## INTRODUCTION

Blending of polymers with thermoplastic elastomers has generated considerable interest owing to desirable improvement in certain properties useful for various specific applications. Among the thermoplastic elastomers, styrene-butadiene-styrene triblock copolymer (SBS) has been a widely used thermoplastic elastomer for this purpose. A modified version of SBS (obtained by hydrogenation of the butadiene block), viz., styrene-ethylene butylene-styrene block copolymer (SEBS) is described<sup>1,2</sup> to possess some superior properties than the SBS. Reports on the use of SEBS in blends with polystyrene and high density polyethylene, and in development of thermoplastic interpenetrating networks have recently appeared in the literature.<sup>3,4</sup> We have reported some studies on the blends of SEBS with isotactic polypropylene (PP) which include the melt rheological<sup>5</sup> and crystallization<sup>6</sup> behaviors of this blend.

Melt rheological behavior of PP/SEBS blends showed<sup>5</sup> lowering of softening temperature, melt viscosity, melt elasticity, and the tendency of melt fracture of PP on blending with SEBS, which implies improvement in the processability of PP on blending with SEBS. Effect of blending with SEBS on the crystallization of PP appeared<sup>6</sup> as the nonlinear (showing maxima

or minima around a certain blend composition) decrease in degree of crystallinity and increase in crystallite size distribution with increase of SEBS content of the blend. Nonlinearity in the variation of tensile properties were also found for this blend, and correlations of these properties with crystallinity and crystallite size distribution parameters were found linear in some cases.<sup>6</sup> Furthermore, although the tensile strength and modulus decreased, the impact strength (at ambient temperature) increased considerably with increasing SEBS content of the blend; the increase was insignificant at lower SEBS content (up to 10 wt %) and quite rapid at higher SEBS content. Such a behavior would be expected because, in addition to the properties of the matrix, the tensile properties would be greatly influenced by the adhesion of the two phases, whereas in the impact behavior the rubbery inclusions may play effectively their role of arresting the passage of impact fracture even in the case of poor interfacial adhesion.

In this article we present a study of the tensile properties of PP/SEBS blend in the yield region. Three different types of samples, viz., (i) solution-blended compression-molded, (ii) melt-blended compression-molded, and (iii) melt-blended injection-molded, are studied in the blend composition range 0–25 wt % SEBS content. These three sets of samples enable one to distinguish the effects of the two blending processes (solution blending and melt blending) and to study the effect of subsequent mixing during injection molding operation in melt-blended samples. The degree of discontinuity in the structure of these three sets of samples is assessed on the basis of the stress concentration parameters of the various theories for two-phase blends or composites.

## EXPERIMENTAL

### Materials

Isotactic polypropylene (PP), Koylene-1730 (MFI = 1.7) and Koylene-3030 (MFI = 3.0) of Indian Petrochemicals Corp., Ltd., and styrene-ethylene butylene-styrene block copolymer (SEBS), Kraton-G 1652 (molecular weights  $8 \times 10^3$ ,  $39 \times 10^3$ , and  $8 \times 10^3$  of S, EB, and S blocks, respectively) of Shell Chemical Co. were used.

### Preparation of Samples

PP/SEBS blends, of compositions 5, 10, 15, 20 and 25 wt % SEBS content, were prepared by (i) solution blending and (ii) melt blending techniques.

Solution blending was done, according to the method described elsewhere,<sup>5</sup> in xylene at 80°C using methanol as precipitating agent. Koylene-1730 grade of PP was used for solution blending.

Melt blending, in a single screw extruder Betol 1820, was done at the screw rpm 40 and temperature profile 200, 210, 220, and 220°C of the first, second, third, and the die zones, respectively. Koylene-3030 grade of PP was used in melt blending owing to its better matching melt flow index with SEBS sample.

Dumbbell shaped specimens for tensile testing, of size conforming with

ASTM-D638 Type 1, were prepared (i) by injection molding using a mold of specific sample shape and dimensions, or (ii) by compression molding into flat sheets and punching out the specimens of specific shape and dimensions. The PP sample was passed through identical operations in extruder before the molding, to have similar thermal history as the other blend samples of the respective sets.

Compression moulding was done on a hydraulic press at 180°C, using 300 kg/cm<sup>2</sup> pressure. Samples were cooled under ambient conditions.

Injection molding, on a Windsor injection molding machine, at injection pressure 600 kg/cm<sup>2</sup>, injection rate 4 cm/s, using the temperature profile, 200°C, 210°C, and 210°C of first, second zones, and the nozzle, respectively.

### Measurements

Tensile properties were measured on an Instron Universal Tester (model 1121) at ambient conditions using gauge length 5 cm and crosshead speed 5 cm/min. A minimum of five samples were tested in each case, and the deviation of data around mean values was less than 5%.

Scanning electron microscopy of fracture surface of the cryogenically fractured samples was done on a Cambridge Instruments scanning electron microscopy (Stereoscan S4-10). Samples were etched in xylene at room temperature to remove the SEBS phase.

## RESULTS AND DISCUSSION

### Yield Peak

Stress-strain curves in the yield region are shown in Figure 1 for the three sets of samples, viz., (1) solution-blended compression-molded (SBCM), (2) melt-blended compression-molded (MBCM), and (3) melt-blended injection-molded (MBIM).

PP shows a sharp yield peak whose width differs in the three PP samples used in these three sets of samples. PP of set 1 has a narrower yield peak than the PP of sets 2 and 3. This difference in peak width is apparently due to the different grades of PP used for the melt-blended and solution-blended sample sets (see the Experimental section). In addition, there appears some difference in the peak width and also the yield stress arising due to the processing operation (i.e., the compression and injection molding), as apparent from the comparison of PP Samples of sets 2 and 3. Though the origin of the observed differences in the yield peak of PP in these three sets may be ascertained only after additional investigations, the changes produced in the yield peak of PP on blending with SEBS are quite similar in each of the three sets of samples. Our subsequent discussion is based on these changes.

Blending of PP with SEBS, in general, increases the peak width and decreases the yield stress over the entire studied range of blend composition. In solution-blended samples, however, some irregularity in peak-width variation was observed around 10–15% SEBS content, which was incidentally

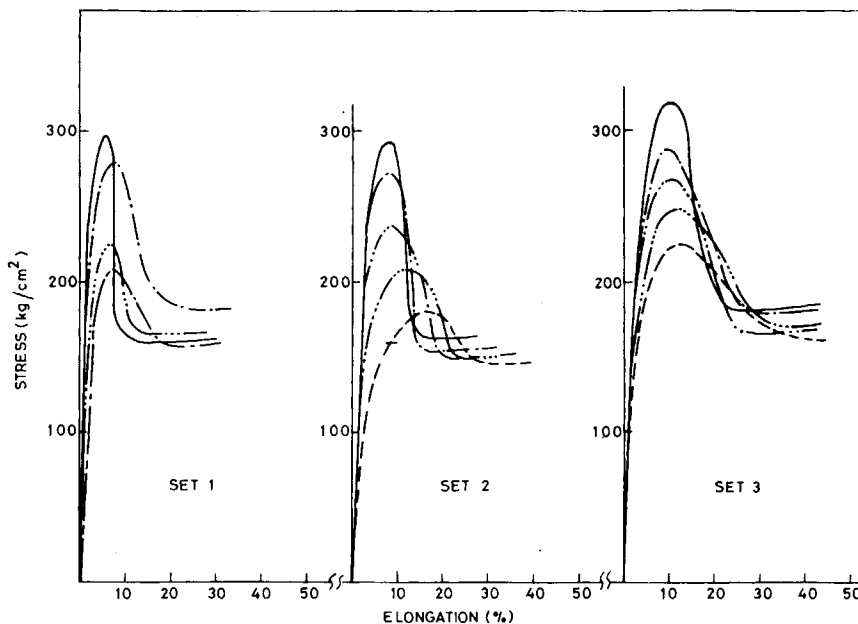


Fig. 1. Stress-strain curves in the yield region of the PP/SEBS blends. Set 1, solution-blended compression-molded; Set 2, melt-blended compression-molded; Set 3, melt-blended injection-molded: (—) PP; (---) 5% SEBS; (- · - ·) 10% SEBS; (· · · ·) 15% SEBS; (- - -) 20% SEBS; (- - -) 25% SEBS.

accompanied by erratic sample breakage in this range for blend samples of set 1. Some additional information useful for understanding this irregularity in solution-blended samples is that these solution-blended samples showed minima in melt viscosity and a sharp decrease in melt elasticity and the simultaneous occurrence of highly deformable small and less deformable large domains of SEBS phase in the region around 10% SEBS content.<sup>5</sup> Broadening of yield peak, in the literature,<sup>7,8</sup> has been attributed to the poor-adhesion characteristics of the blend on the basis of the data on polycarbonate (PC)/high density polyethylene (HDPE) (poor adhesion type) blends. On this basis the broadening of yield peak may suggest a decrease in interphase adhesion with increasing SEBS content in these blends, which seems not well supported by our subsequent discussion. The present blend is different from the above cited blend as one of the components is an elastomer, which might contribute to additional elongation in the yield region of the other component, resulting in the broadening of the yield peak.

### Work of Yield

Stress-strain curve of PP, shown in Figure 1, shows an initial linear increase of stress with strain and gradually develops into the peak and thereafter the stress decreases with increasing elongation up to a point, which is called hereafter "tip" of the yield peak. Beyond this tip the stress increases quite slowly with strain up to the ultimate breaking point occurring at elongations 350–600% for all the samples. Variation of elongation at break and tensile strength with blend composition and their correlations

with crystallinity parameters of PP component are described elsewhere.<sup>6</sup> The stress and strain values corresponding to the yield peak are denoted as yield stress ( $\sigma_y$ ) and yield strain ( $\epsilon_y$ ), respectively. Necking occurs in the region just beyond the tip of the yield peak. Stress-strain curves for the blend samples have qualitatively similar features as those described above for PP.

Area under the stress-strain curve from the origin to the tip of the yield peak (limit indicated through vertical lines drawn in Fig. 2) is a measure of the total energy required for the deformation in yield region, or, in other words, the "work of yield." As apparent from the values shown in Table I, blending of PP with SEBS increases the work of yield by a factor of about 1.5 over the total studied range of blend composition. As shown in Figure 3, this increase is initially rapid at low SEBS content and then approaches a limiting value beyond 20% SEBS content. It may thus be stated on the basis of these results that (i) blending with SEBS makes the yielding of PP more difficult, as it increases the work of yield and (ii) blending with SEBS increases the yield strain, as well as the elongation up to the tip of yield peak, and decreases the yield stress.

This increase of work of yield suggests some role of SEBS inclusions on the yield behavior of PP. In the stress-strain curve of SEBS, no yield behavior was observed. If the blend is assumed to be a two-phase continuous system (i.e., perfect adhesion between the two phases), then the elastomer extension may overlap the yield behavior of PP, and thus the yield peak may widen and get suppressed, as is observed in this case. The role of elastomer component is apparent also in the increase of yield strain with the SEBS content of the blend. However, the decrease of modulus (see Table I) is quite small to justify any significant contribution of the elastomer

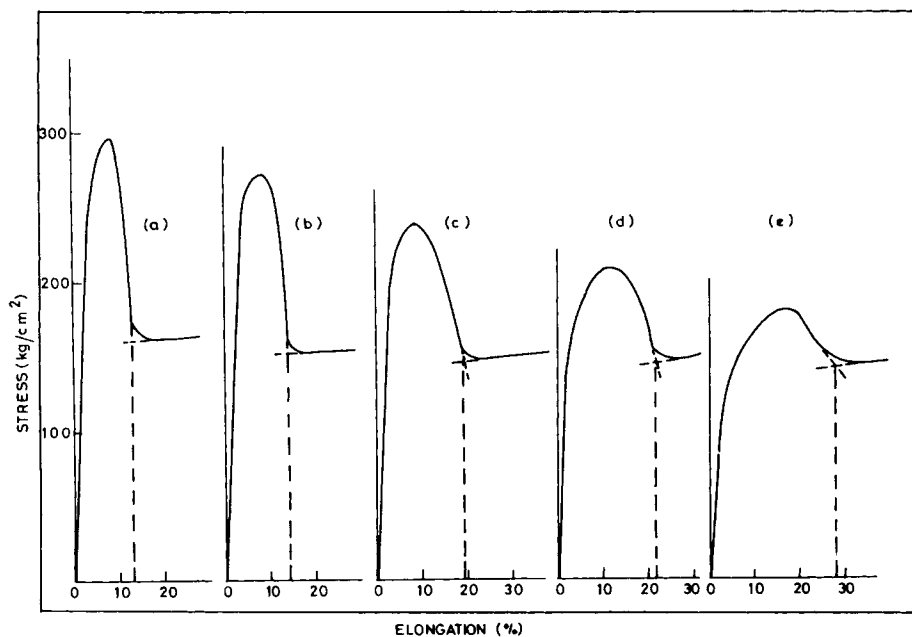


Fig. 2. Change in shape of the stress strain curve in the yield region with varying blend composition, (wt % SEBS): (a) 0; (b) 5; (c) 10; (d) 15; (e) 25.

TABLE I  
Values of Various Tensile Parameters for PP/SEBS Blends

Blend classification	Blend composition (wt % SEBS)	1% secant modulus (kg/cm <sup>2</sup> ) × 10 <sup>-1</sup>	Tensile strength (kg/cm <sup>2</sup> )	Yield stress (kg/cm <sup>2</sup> )	Area under yield peak (arbitrary unit)
Solution-blended compression-molded (SBCM), set 1	0	18.0	213	298	14.2
	5	14.5	220	285	15.0
	10	13.4	—	250	—
	15	11.0	203	225	15.0
	20	10.2	196	210	22.6
Melt-blended compression-molded (MBCM), set 2	0	10.2	—	300	21.8
	5	9.0	—	270	23.9
	10	10.0	—	232	28.1
	15	8.0	—	206	29.3
	25	7.0	—	180	31.7
Melt-blended injection-molded (MBIM), set 3	0	8.4	210	320	17.2
	5	7.4	196	290	18.8
	10	7.9	188	273	19.9
	15	6.8	192	248	22.5
	25	6.2	186	220	23.5

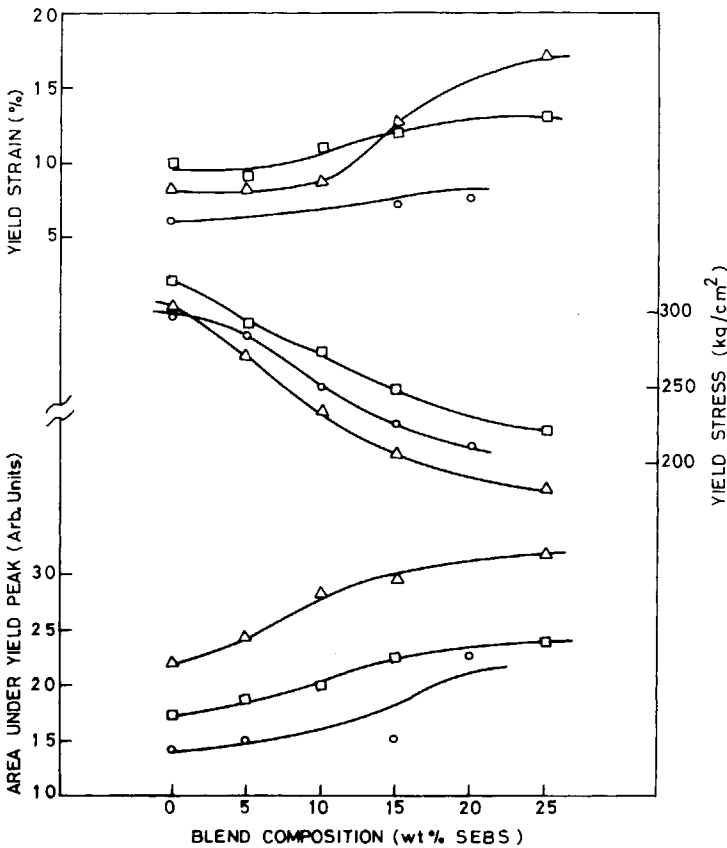


Fig. 3. Variation of the yield stress, yield strain, and area under the yield peak with blend composition for PP/SEBS blends: (○) Set 1; (△) Set 2; (□) Set 3.

phase (SEBS) in it. Also noteworthy is the fact that these modulus values have been found linearly correlated with crystallinity parameters of PP component of the blend.<sup>6</sup>

These results, thus, generate a further curiosity about the role of the elastomer component of this blend. It is well recognized that the continuity in the structure, or the interphase adhesion, is important for any significant role of the dispersed phase in a two-phase blend. This will be explored in the subsequent discussion.

### Shear Bands

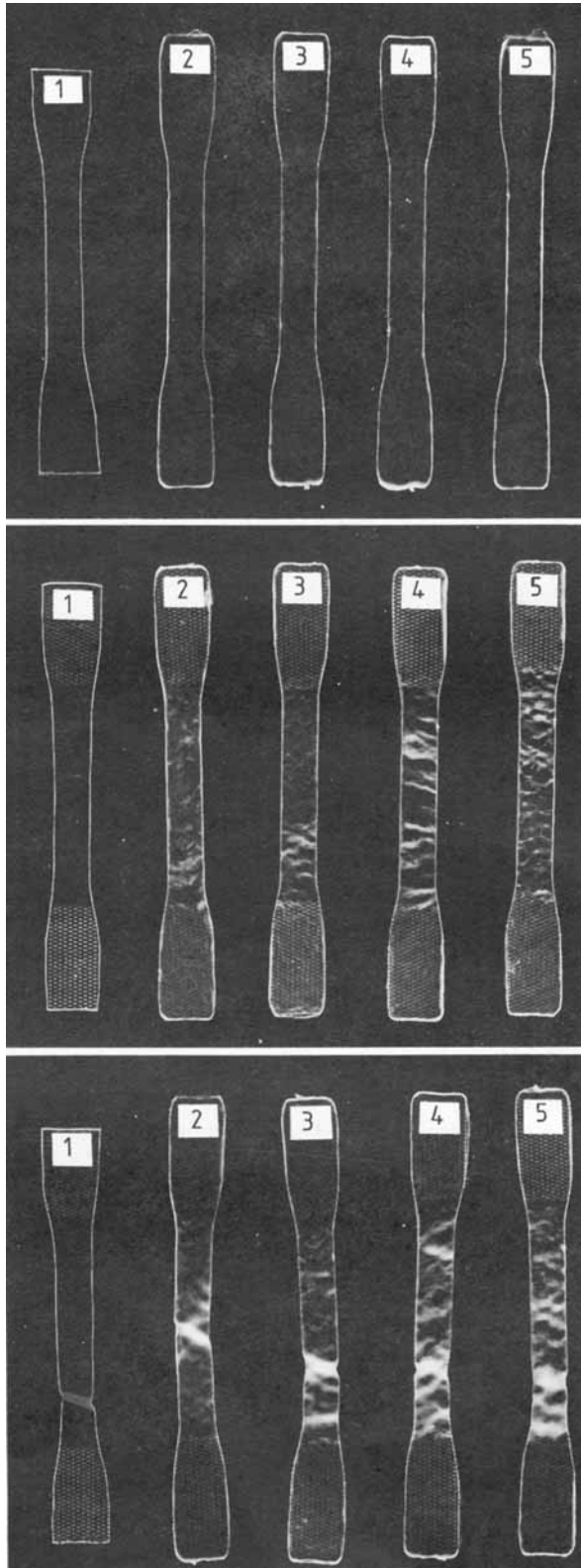
Growth of shear bands during tensile stretching showed some significant differences in the samples of different blend compositions. These observations were made at a slower rate of deformation, viz., 0.2 cm/min, for convenience of observation of gradual changes in shear bands. Observations made during the course of stretching are described in words and illustrated in Figure 4, through photographs of the samples at three stages of stretching, viz., (i) up to the formation of necking zone [Fig. 4(c)], (ii) up to the elongation corresponding to the yield peak position [Fig. 4(b)], and (iii) unstretched [Fig. 4(a)].

During the process of stretching tiny white streaks appeared with their first appearance, depending on the extent of stretching; the higher the SEBS content of the blend, the lower the stretching required for the first appearance of these streaks. On further stretching the streaks developed into lateral shear bands; the number and width of the shear bands increasing with increasing stretching of the sample. Gradually the overlapping of the bands and formation of wider bands occurs, and finally one of these wide bands develops into the necking zone shown in Figure 4(c). The number and surface density of the shear bands increases with increasing SEBS content in the blend samples, while in the PP sample there is only one band which develops into the neck.

Localization of shear deformation into the regions of inhomogeneities of strain (or stress concentration) gives rise to formation of shear microbands which grow in size on further stretching beyond yield point to form bigger bands. These shear bands appear white owing to the refractive index difference between the band and the adjacent underformed polymer. The observed absence of shear bands in unblended PP and their occurrence in all the blend samples, as well as the increasing degree of shear bands with increasing SEBS content of the blend (Fig. 4), indicate that SEBS inclusions give rise to regions of strain inhomogeneities or stress concentration in these blends. Furthermore, unlike crazes, shear bands propagate along lines of zero strain rate at angles different from 90° with direction of stretching. The observed inclination of these bands is close to 60° which is a value calculated from the assumption of transversely isotropic behavior of the strain.

### Analysis of Blend Composition Dependence

Analysis of these yield stress data as a function of blend composition on the basis of some existing theoretical models permits not only the characterization of discontinuity in the structure but also reveals some impor-





tant differences between the three sets of samples, SBCM, MBCM, and MBIM. Before the actual analysis of the data, a brief review of the theories used is presented along with the significance of the parameters characterizing the discontinuity of structure in these different models.

Two most common expressions of composition dependence of mechanical properties of two-phase blends (or composites) are based on the first power [eq. (1)] and two-thirds power [eq. (2)] laws, expressed as

$$\sigma = \sigma_0(1 - \phi) \quad (1)$$

$$\sigma = \sigma_0(1 - \phi^{2/3}) \quad (2)$$

where  $\sigma$  and  $\sigma_0$  denote the given mechanical property (yield stress, tensile strength, etc.) of the blend and the matrix, respectively.  $\phi$  is the volume fraction of the dispersed phase. These power laws originate from the relationship of area fraction and volume fraction of the inclusions.<sup>8,9</sup> For a completely random distribution of the dispersed phase, the first power relationship of area fraction to volume fraction in any randomly chosen plane of fracture is derived on simple mathematical considerations.<sup>9</sup> On the other hand, for the case of spherical inclusions, the two-thirds power law with appropriate weightage factor is derived<sup>9</sup> for any randomly chosen plane. It is, however, difficult to decide which of these laws do really hold for a given system. However, in some experiments based on the image analysis of SEM pictures of more than 100 fracture surfaces of each sample, Kunori and Geil<sup>8</sup> showed the validity of both first power and two-thirds power relationships of area fraction and volume fraction for the same blend depending on the composition or the shape of the inclusions.

The realistic features of deformation and fracture, such as the stress concentrations at the narrow portions of the matrix at the inclusion-matrix interface were incorporated in these power laws in various different ways. In the two-thirds power law Nielsen<sup>10</sup> suggested the use of a parameter  $S$ , eq. (3), while Nicolais and Narkis<sup>11</sup> suggested the use of a weightage factor 1.21, eq. (4). In the first power law Piggott and Leidner<sup>9</sup> suggested the incorporation of two parameters  $A$  and  $B$ , eq. (5):

$$\sigma = \sigma_0(1 - \phi^{2/3})S \quad (3)$$

$$\sigma = \sigma_0(1 - 1.21 \phi^{2/3}) \quad (4)$$

$$\sigma = \sigma_0(A - B\phi) \quad (5)$$

According to Nielsen's definition, the maximum value of parameter  $S$  is unity for the "no stress concentration effect" (or perfect adhesion) case, and the lower the value of  $S$ , the greater the stress concentration effect (or poorer the adhesion).

The parameter 1.21 in Eq. (4), which is viewed by some authors<sup>8</sup> as a parameter equivalent to the stress concentration parameter  $S$  of Nielsen,

---

Fig. 4. Photographs showing the changes in shear bands during the course of stretching: (a) unstretched; (b) stretched up to the yield peak; (c) stretched up to the necking. Numbers marked denote the blend composition (wt % SEBS), as follows: (1) 0; (2) 5; (3) 10; (4) 15; (5) 25.

has been shown by Piggott and Leidner to be the outcome of the spherical shape of the inclusions.

In the two-parameter expression of the first power law [eq. (5)], the parameter  $A$  is stated<sup>9</sup> to represent the weakening of the structure due to stress concentration effect, while the parameter  $B$  takes account of volume fraction proportionality of the strength. Looking back at eqs. (3) and (4), we find that in eq. (3) the parameter  $S$  plays the role of both the parameters, while in eq. (4) the parameter 1.21 is operative only on the volume fraction term.

Although it is possible to obtain agreement of experimental data which any of these theoretical models with suitable choice of the values of the parameters, the present analysis for evaluation of the stress concentration parameters in these and some other expressions given below is aimed essentially to distinguish the stress concentration effects in the various samples. Relative evaluation of the suitability of any one expression or the other to the present system is an outcome of this analysis.

Furthermore, we thought it worthwhile to incorporate the stress concentration effect in the first power law through the use of a parameter  $S'$ , in a manner analogous to Nielsen's expression, leading to the following relation:

$$\sigma = \sigma_0(1 - \phi)S' \quad (6)$$

where  $S'$  can acquire its maximum value unity for the case of "no stress concentration effect," and its lower value implies greater stress concentration effect. This expression, clearly, is a special case of the two-parameter expression [eq. (5)], representing  $A = B$ .

Another way of representing the behavior of a poor adhesion type blend is to consider the two-phase system as a matrix with pores or voids. The material filling the pores is the dispersed phase which remains inoperative in playing a direct role in influencing the mechanical properties of the blend due to nonadhesion at the interphase boundary. Explanation of mechanical properties in terms of porosity is widely used for nonpolymeric materials such as sintered porous metals and ceramics.<sup>12</sup> Nielsen<sup>13</sup> suggested the applicability of this porosity concept to polymer matrix with voids or holes, and its use for polymer blends is also illustrated.<sup>8</sup> According to this theory, the specific change  $d\sigma/\sigma$  in a property of the system is directly proportional to the porosity  $P$ , or

$$-\frac{d\sigma}{\sigma} = aP \quad (7)$$

where  $a$  is the proportionality constant, and the negative sign implies the decrease of the property with increase of porosity. Replacing the total porosity with volume fraction  $\phi$  of the inclusion leads to the following expression for the two-phase system:

$$\sigma = \sigma_0 \exp(-a\phi) \quad (8)$$

The relationship of the parameter  $a$  of eq. (8) with the stress concentration

effect is suggested<sup>8</sup> from the similarity of the effects of tensile deformation rate and stress concentration on the value of  $a$ ; the higher the stress concentration, the higher will be the value of  $a$ .

In order to explore the applicability of first power or two-thirds power law to the present system, plots of  $\log[(\sigma_0 - \sigma)/\sigma_0]$  vs.  $\log \phi$  from these yield stress data are shown in Figure 5. The slope of this plot gives the value of the power law exponent according to eqs. (1) and (2). Curvature, implying change of slope with blend composition, is apparent in all cases, except the case of samples of set 3 (i.e., MBIM), where the curvature is undetectably small. Values of slopes corresponding to the two linear portions, shown by broken lines, of each of these curves are shown in Table II. At high volume fractions ( $\phi > 0.09$ ) the slopes in all these cases are quite consistent with the two-thirds power law, while at the lower volume fractions the data seem to approach the first power law. However, in the low volume fraction region, the slope is considerably greater than unity for the set 1 samples, and sufficiently close to, or in-between, both unity and two-thirds exponent values for the set-3 samples (which makes difficult the distinction between the applicability of first power or two-thirds power law). Better suitability of the first power law than the fractional power laws is reported by some authors for the strength<sup>14</sup> and yield stress<sup>15,16</sup> of composites. In this analysis the stress concentration parameters [shown in eqs. (3)–(6)] were not taken into account; hence the information obtained may be subject

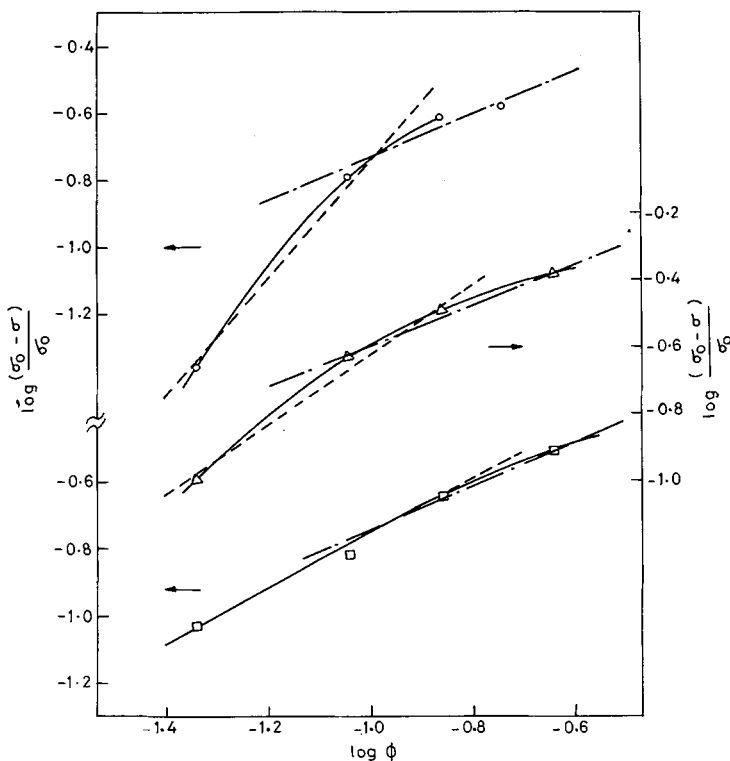


Fig. 5. Variation of  $\log(\sigma_0 - \sigma)/\sigma_0$  as a function of  $\log \phi$ : (○) Set 1; (△) Set 2; (□) Set 3.

TABLE II  
Slopes of the Two Linear Portions of the  $\log(\sigma_0 - \sigma)/\sigma_0$  vs.  $\log \phi$  Plots

Sample	Slope	
	At $\phi < 0.09$	At $\phi > 0.09$
Set 1 (SBCM)	1.70	0.64
Set 2 (MBCM)	1.04	0.61
Set 3 (MBIM)	0.82	0.65

to further modification on incorporation of the other parameters, as described subsequently.

Agreement of these data with both first power and two-thirds power law expressions [eqs. (3) and (6)] can be achieved at each individual blend composition by using appropriate values of  $S$  or  $S'$ , shown in Table III. These values of  $S$  are, however, greater than unity, which is in contradiction with the basic definition of this parameter stated above. These greater than unity values might be an indication of either a necessity of using the exponent of  $\phi$  greater than  $2/3$  or of using an additional term, like the term  $A$  of eq. (5), in Nielsen's equation [eq. (3)].

Comparisons of theoretical curves with the experimental data are presented in Figures 6–8. In the case of Nielsen's equation [eq. (3)] the agreement was good in the high volume fraction region ( $\phi > 0.09$ ) with values of  $S$  quite close to the mean of the values for the samples containing 10% or more SEBS (shown in Table III). In the region of lower volume fraction the agreement was not good, presumably due to the deviation of the system from the two-thirds power law.

In the case of first power law expression with parameter  $S'$  [eq. (6)], the comparison of experimental data with two theoretical lines corresponding to  $S' = 1$  and  $S' = 0.88$  (set 1), 0.80 (set 2), 0.90 (set 3) (Figs. 6–8) suggests that the system undergoes a transition from the state of "no stress concentration effect" to a state with significant stress concentration effect, on increasing the volume fraction of SEBS phase. The volume fraction corresponding to the midpoint of this transition increases in the following order: MBCM < MBIM  $\leq$  SBCM.

TABLE III  
Values of Stress Concentration Parameters,  $S$  [eq. (3)] and  $S'$  [eq. (6)], Fitting These Data at Individual Compositions of Blend

Blend composition		$S$			$S'$		
wt SEBS	% $\phi$	SBCM	MBCM	MBIM	SBCM	MBCM	MBIM
0	0	—	—	—	—	—	—
5	0.0452	1.09	1.03	1.00	1.00	0.94	0.94
10	0.0909	1.05	0.97	1.07	1.92	0.85	0.91
15	0.1371	1.03	0.94	1.06	0.88	0.80	0.90
20	0.1837	1.04	—	—	0.86	—	—
25	0.2308	—	0.96	1.10	—	0.78	0.89
Mean value <sup>a</sup>		1.04	0.96	1.08	0.89	0.81	0.90

<sup>a</sup> Mean taken for the last three values, i.e., for the samples with SEBS content  $\geq 10$  wt %.

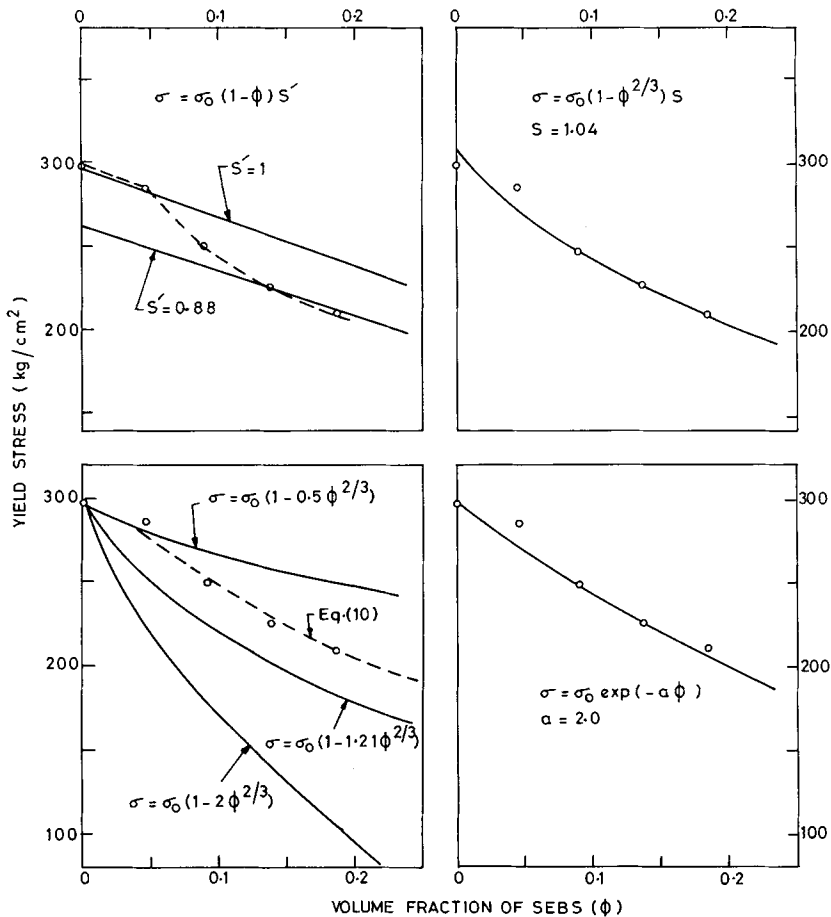


Fig. 6. Comparison of the experimental data with various theoretical relationships for the blend composition dependence of yield stress for solution-blended compression-molded samples of PP/SEBS blend.

A comparison of  $S'$  values in the high volume fraction state, suggests that the stress concentration effect, in these three sets of samples, increases in the following order: MBIM < SBCM < MBCM.

Considering the difference between the results of set 1 (SBCM) and set 3 (MBIM) negligible in comparison to their differences with the set 2 (MBCM), it may be stated that the greater the tendency of stress concentration effect, the smaller the volume fraction of inclusions at which the transition occurs from the state of continuous structure to the state with discontinuities in the structure.

The Nicolais and Narkis equation [eq. (4)] shows some disagreement with these experimental data (Figs. 6-8). It is further noted that an alternative choice for the parameter 1.21 in this expression does not lead to any desirable agreement, as illustrated in the figures by the choice of two values 0.5 and 2.0 in place of 1.21. However, the parallelism of the variation of experimental data and the theoretical curve with parameter 1.21 is remarkable, which suggests the need of an additional additive term in this

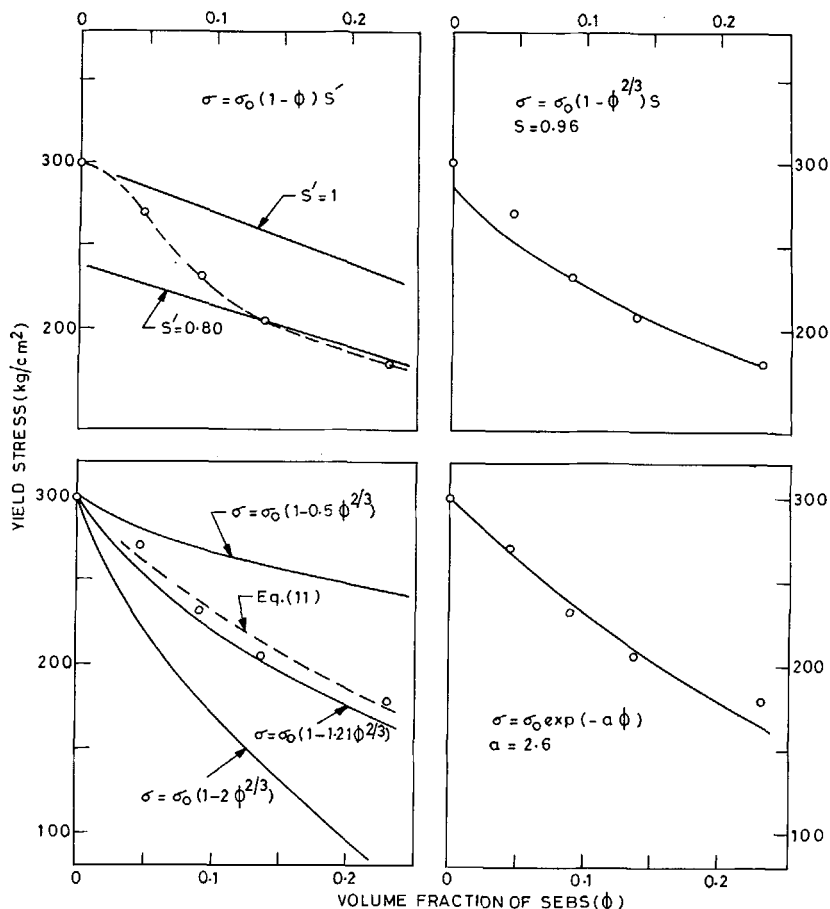


Fig. 7. Comparison of the experimental data with various theoretical relationships for the blend composition dependence of the yield stress for melt-blended compression-molded samples of PP/SEBS blend.

expression [eq. (4)]. Such an additive term, incorporated like the parameter  $A$  in eq. (5), modifies the eq. (4) to the following form:

$$\sigma = \sigma_0(A' - 1.21\phi^{2/3}) \quad (9)$$

Evaluation of the parameter  $A'$  from these data leads to following relationships for the three sets of samples:

$$\sigma = \sigma_0(1.091 - 1.21\phi^{2/3}) \quad \text{for SBCM} \quad (10)$$

$$\sigma = \sigma_0(1.033 - 1.21\phi^{2/3}) \quad \text{for MBCM} \quad (11)$$

$$\sigma = \sigma_0(1.098 - 1.21\phi^{2/3}) \quad \text{for MBIM} \quad (12)$$

These expressions are represented by dotted line curves in Figures 6–8 to show their agreement with experimental data. In analogy with the significance of the similar parameter  $A$  occurring in Piggott and Leidner's expres-

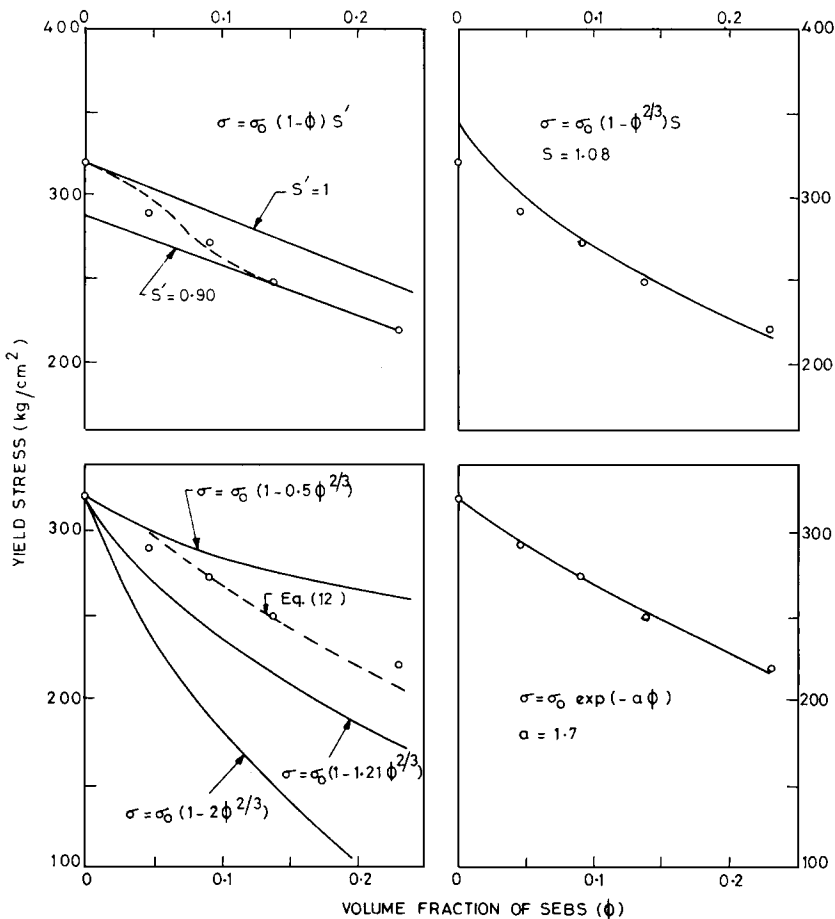


Fig. 8. Comparison of the experimental data with various theoretical relationships for the blend composition dependence of yield stress for melt-blended injection-molded samples of PP/SEBS blend.

sion of first power law [eq. (5)], if we consider the lower value of the parameter  $A'$  in eq. (9) to represent greater weakening of the structure due to stress concentration, then these values of  $A'$  suggest the same order of increase of stress concentration effect as found by other expressions, viz., MBIM < SBCM < MBCM.

The expression of porosity model [eq. (8)] seems to fit quite satisfactorily with these data as shown in Figures 6–8 with the values of the parameter  $a$ : 2.0 (for SBCM), 2.6 for (MBCM), and 1.7 (for MBIM). The agreement is quite good in the entire range of blend composition studied. As stated above, the higher the value of  $a$ , the greater the stress concentration. Hence, the observed order of increase of  $a$ , viz., MBIM < SBCM < MBCM, indicates the increase of stress concentration effect in the same order. This order of increase of stress concentration effect in these three sets of samples is consistent with that obtained from the stress concentration parameters of eqs. (3) and (6).

### Scanning Electron Microscopy

Scanning electron micrographs of fracture surfaces of samples, fractured at liquid-air temperature and etched in xylene to dissolve out the SEBS component, are shown in Figures 9 and 10 for SBCM and MBIM sets of samples of various blend compositions and at a constant magnification. Owing to the irregular shapes and varying sizes of the dispersed phase domains, comparison of the state of dispersion (or average domain size) for the three sets of samples (viz., SBCM, MBCM and MBIM) could not be possible from these SEM studies. However, information based on shapes and sizes of the SEBS domains at various blend compositions, described below, supports some of the findings stated in a previous section.

These micrographs show irregular shapes of the inclusions (SEBS domains). The domains are quite small in the case of samples with the lowest SEBS content (i.e., 5%). Occurrence of larger domains (about 50  $\mu\text{m}$  or more, lengthwise) is apparent at SEBS content 10% or more. The transition, predicted on the basis of the values of stress-concentration parameter  $S'$  in eq. (6), from a continuous structure (i.e., no stress concentration effect) to a discontinuous structure (i.e., significant stress concentration effect) seems supported by the observed domain sizes. At lower SEBS content, where the

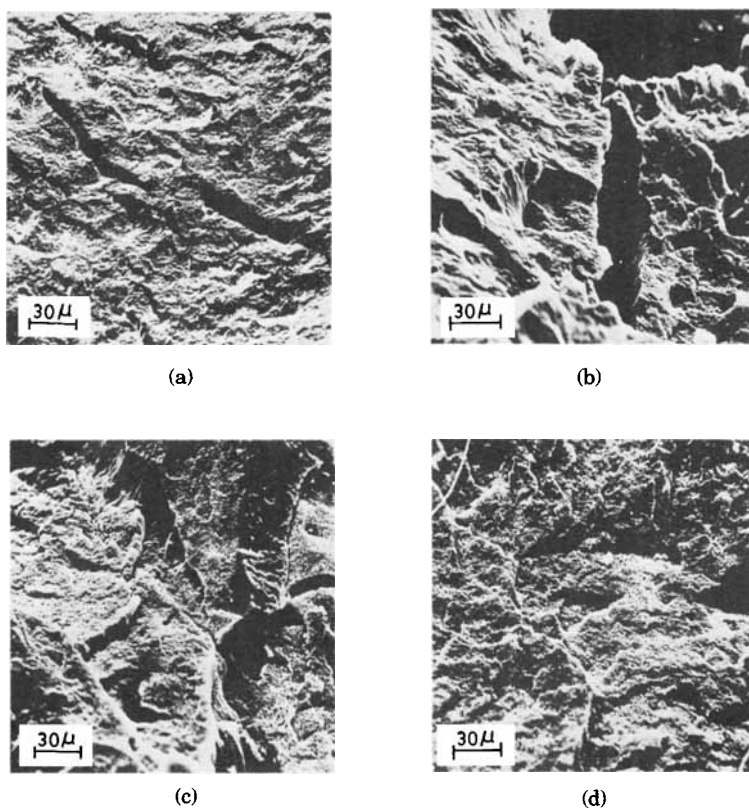


Fig. 9. Scanning electron micrographs of cryogenically fractured (etched with xylene) surfaces of the solution blended compression molded samples of PP/SEBS blend of varying composition (wt % SEBS): (a) 5; (b) 10; (c) 15; (d) 20.



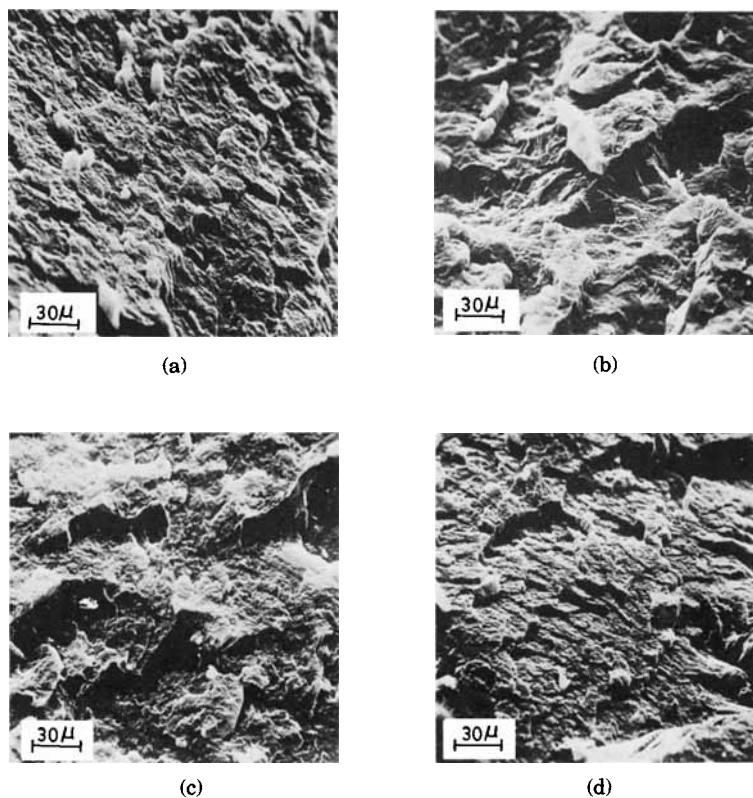


Fig. 10. Scanning electron micrographs of cryogenically fractured (etched with xylene) surfaces of the melt-blended injection-molded samples of PP/SEBS blend of varying composition (wt % SEBS): (a) 5; (b) 10; (c) 15; (d) 25.

domains are small, the system shows lower stress concentration, while at SEBS contents 10% or more the bigger domains as well as their irregular shapes with sharp corners might be the cause of the significant stress concentration effect shown by the system. It is believed by various authors<sup>8,9,14,17</sup> that: (i) the greater the size of inclusions, the greater the stress concentration; (ii) the stress concentration is lower for the case of rounded or spherical inclusions than the inclusions with sharp corners or irregular shapes.

These micrographs also show that the mixing of the two phases produces more rounded boundaries with less sharp corners of the inclusions in the case of MBIM (which involved two mixing processes, one during blending and the other during injection moulding) samples (Fig. 10) than the SBCM samples (Fig. 9). This observation provides a qualitative support to the lower stress concentration effect in MBIM than SBCM sets of samples, found in the above analysis of yield stress data.

### Effect of Injection Molding

As shown from the analysis of yield stress data, the stress concentration effect described on the basis of all the four parameters,  $S$  [eq. (3)],  $S'$  [eq. (6)],  $a$  [Eq. (8)] and  $A'$  [Eq. (9)], increases in the following order for the three sets of samples: MBIM < SBCM < MBCM. This implies that the solution

blending produces better mixing than the melt blending in an extruder and that the subsequent mixing during injection molding process improves the mixing to an extent that its tensile properties become superior to the solution-blended compression-molded samples.

This behavior of the three sets of samples indicates that the state of dispersion of the two phases plays an important role in the tensile properties of PP/SEBS blend. SEM studies, which did not enable evaluation of the overall state of dispersion, showed some effect of injection molding on the shapes of bigger domains as well as the simultaneous occurrence of smaller domains and bigger domains. This suggests that the observed differences in stress concentration effect of the three sets of samples might be accounted for by (i) relative abundance of bigger or smaller sized domains and/or (ii) rounded shapes (with less sharp corners) of the SEBS domains.

Finally, it may be stated, in passing, that the injection-molded samples showed lower modulus and almost same tensile strength than the compression-molded samples. The melt-blended compression-molded (MBCM) samples, which had the highest stress concentration or the weakest structure, showed some erratic behavior in the breaking of these samples which did not enable the determination of tensile strength with accuracy (not included in Table I) for this set of samples.

This study, though, shows a decrease in tensile yield stress of PP on blending with SEBS, provides useful information about the structure of this blend, and presents a comparative evaluation of the various processing operations on the structure and properties of this blend. Like the various rubber-toughened plastics, for which the decrease in tensile strength is a common feature, the PP/SEBS blend shows considerable improvement in impact strength and dynamic mechanical damping behavior, which will be dealt with in a subsequent paper.<sup>18</sup>

## CONCLUSIONS

Blending with SEBS lowers the yield stress, increases yield strain, widens the yield peak, and increases the work of yield of PP. Stress whitening characteristic of shear band formation is observed during early stages of tensile deformation.

As regards the first power and two-thirds power laws, the yield stress of this blend shows first power law type behavior at lower SEBS contents (volume fraction  $< 0.09$ ) and two-thirds power law type behavior at higher SEBS content. The one-parameter incorporation of stress concentration effect in these power laws did not describe satisfactorily the behavior of this blend, over the whole studied range, with a single value of the parameter. However, the porosity model with one stress concentration parameter was found adequate to describe the behavior of this blend over the whole range. In other models the two-parameter expressions were expected to be more appropriate.

This system undergoes a transition from the state of continuous structure (zero stress concentration) to a state of discontinuous structure (occurrence of stress concentration) at around 5% SEBS content. Increase of stress concentration effect is accompanied by an increase in size of SEBS domains.

Further mixing during injection molding of the melt-blended samples lowers the stress concentration effect, presumably due to more homogenous dispersion resulting into smaller size of the SEBS domains. Mixing of the two phases was better in the solution blending than melt blending in an extruder.

### References

1. P. Dreyfuss, L. J. Fetters, and D. R. Hansen, *Rubber Chem. Technol.*, **53**, 728 (1980).
2. W. P. Gergen and S. Davison, U.S. Pat. 4,107,130 (1978).
3. C. R. Lindsey, D. R. Paul, and J. H. Barlow, *J. Appl. Polym. Sci.*, **26**, 1 (1981).
4. D. L. Seigfried, D. A. Thomas, and L. H. Sperling, *J. Appl. Polym. Sci.*, **26**, 177 (1981).
5. A. K. Gupta and S. N. Purwar, *J. Appl. Polym. Sci.*, **29**, 1079 (1984).
6. A. K. Gupta and S. N. Purwar, *J. Appl. Polym. Sci.*, **29**, 1545 (1984).
7. T. Kunori and P. H. Geil, *J. Macromol. Sci. Phys.*, **B(18)**, 93 (1980).
8. T. Kunori and P. H. Geil, *J. Macromol. Sci. Phys.*, **B(18)** 135 (1980).
9. M. R. Piggott and J. Leidner, *J. Appl. Polym. Sci.*, **18**, 1619 (1974).
10. L. E. Neilsen, *J. Appl. Polym. Sci.*, **10**, 97 (1966).
11. L. Nicolais and M. Narkis, *Polym. Eng. Sci.*, **11**, 194 (1971).
12. E. M. Passmore, R. M. Spriggs, and T. Vasilos, *J. Am. Ceram. Soc.*, **48**, 1 (1965).
13. L. E. Nielsen, *J. Compos. Mater.*, **1**, 100 (1967).
14. S. Sahu and L. J. Broutman, *Polym. Eng. Sci.*, **12**, 91 (1972).
15. G. W. Brassell and K. B. Wischmann, SPE Regional Technical Conference on Advances in Reinforced Thermoplastics, El Segundo, Calif., Paper 1, 1972.
16. O. Ishai and L. J. Cohen, *J. Comp. Mater.*, **2**, 302 (1968).
17. A. A. Griffiths, *Proc. Roy. Soc., London*, **A221**, 163 (1920).
18. A. K. Gupta and S. N. Purwar, *J. Appl. Polym. Sci.*, to appear.

Received November 8, 1983

Accepted February 19, 1984